Multi-Period Active Distribution Network Planning Using Multi-Stage Stochastic Programming and Nested Decomposition by SDDIP

Tao Ding, *Senior Member, IEEE*, Ming Qu, *Student Member, IEEE*, Can Huang, *Senior Member, IEEE*, Zekai Wang, *Student Member, IEEE*, Pengwei Du, *Senior Member, IEEE*, and Mohammad Shahidehpour, *Fellow, IEEE*

***Abstract*—This paper presents a multi-period active distribution network planning (ADNP) with distributed generation (DG). The objective of the proposed ADNP is to minimize the total planning cost, subject to both investment and operation constraints. The paper proposes a multi-stage stochastic optimization model to address DG uncertainties over several periods, in which the decisions are made sequentially by only using the present-stage information. A nested decomposition method is proposed which applies the stochastic dual dynamic integer programming (SDDIP) method to address computational intractabilities of the proposed ADNP approach. The presented numerical results and discussions on a 33-bus distribution system and a large-scale 906-bus system verify the effectiveness of the proposed ADNP method and its solution method.**

***Index Terms*—Distribution network planning, uncertainty, distributed energy resources, multi-stage stochastic programming.**

Nomenclature

Name Abbreviation

LN, *ST*, *TR*, *DG*	Denote transmission lines, substations, transformers, and distributed generators (DGs).

Indices

i, j, k, r	Indices of buses.
t, h	Indices of periods.
V	Indices of segments in piecewise linearization.

Sets

Ω^N/Ω^B	Set of buses/lines.
$\Omega^{LN}, \Omega^{ST}, \Omega^{TR}, \Omega^{DG}, \Omega^{LD}$	Set of transmission lines, substations, transformers, DGs and load buses.

Parameters

R_{jk}/X_{jk}	Resistance/ Reactance of line (j, k).
μ	Maximum penetration rate of DGs.
σ	Annual interest rate.
$P_{k,t}^{LD}, Q_{k,t}^{LD}$	Active and reactive loads at bus k at period t.
N^b	Number of buses.
T	Number of planning periods.
θ_k	Power factor angle of the load at bus k.
$\delta_{kr,t}^{LN}, \delta_{k,t}^{ST}, \delta_{kr,t}^{TR}, \delta_{k,t}^{DG}$	Investment prices of (k, r)-th line, k-th substation, (k, r)-th transformer and k-th DG at period t.
$\gamma_{kr,t}^{LN}, \gamma_{k,t}^{ST}, \gamma_{kr,t}^{TR}, \gamma_{k,t}^{DG}$	Maintenance prices of (k, r)-th line, k-th substation, (k, r)-th transformer and k-th DG at period t.
$\chi_{kr}^{LN}, \chi_{k}^{ST}, \chi_{kr}^{TR}, \chi_{k}^{DG}$	Equipment lifetime of (k, r)-th line, k-th substation, (k, r)-th transformer and k-th DG.
${\lambda_t}^{ST}$	Electricity purchase price at period t.
$U_k^{\min}, U_k^{\max}, U_k^0$	Lower and upper bounds of voltage magnitude at bus k; the specified voltage at substation k.
$I_{kr}^{LN,\min}, I_{kr}^{LN,\max}$	Lower and upper bounds of current on (k, r)-th transmission line.
$I_{kr}^{TR,\min}, I_{kr}^{TR,\max}$	Lower and upper bounds of current on (k, r)-th transformer.
$S_{kr}^{LN,\max}, S_{kr}^{TR,\max}$	Apparent power capacities on (k, r)-the transmission line and transformer.
$P_k^{ST,\max}, Q_k^{ST,\max}$	Active and reactive power capacities of k-th substation.
$P_k^{DG,\max}, S_k^{DG,\max}$	Active and apparent power capacities of k-th DG.
M	A large number.

Manuscript received April 15, 2020; revised August 9, 2020 and October 3, 2020; accepted October 17, 2020. Date of publication October 21, 2020; date of current version April 19, 2021. This work was supported in part by National Key Research and Development Program of China under grant 2016YFB0901900, in part by National Natural Science Foundation of China under Grant 51977166, in part by China Postdoctoral Science Foundation under Grant 2017T100748, in part by Natural Science Foundation of Shaanxi Province under Grant 2020KW-022, and in part by the auspices of U.S. Department of Energy by Lawrence Livermore National Laboratory under contract DE-AC52-07NA27344 with IM release number LLNL-JRNL-815905. Paper no. TPWRS-00623-2020. *(Corresponding author: Tao Ding.)*

Tao Ding, Ming Qu, and Zekai Wang are with the Department of Electrical Engineering, Xi'an Jiaotong University, Xi'an 710049, China (e-mail: tding15@mail.xjtu.edu.cn; quming@stu.xjtu.edu.cn; dcxxx212@stu.xjtu.edu.cn).

Can Huang is with the Lawrence Livermore National Laboratory, Livermore, CA 94550 USA (e-mail: can7huang@gmail.com).

Pengwei Du is with the Electric Reliability Council of Texas, Austin, TX 76574 USA (e-mail: pengwei.du@ercot.com).

Mohammad Shahidehpour is with the ECE Department, Illinois Institute of Technology, Chicago, IL 60616 USA (e-mail: ms@iit.edu).

Color versions of one or more of the figures in this article are available online at https://ieeexplore.ieee.org.

Digital Object Identifier 10.1109/TPWRS.2020.3032830

N	Number of sampled scenarios.
N_t	Number of sampled scenarios at period t.
N_v	Number of segments for linearization.

Variables

$x^{LN}_{kr,t}, x^{ST}_{k,t}, x^{TR}_{kr,t}, x^{DG}_{k,t}$	Binary variables representing the investment decisions of (k, r)-th line, k-th substation, (k, r)-th transformer and k-th DG at period t.
$y^{LN}_{kr,t}, y^{ST}_{k,t}, y^{TR}_{kr,t}, y^{DG}_{k,t}$	Binary variables representing the operation decisions of (k, r)-th line, k-th substation, (k, r)-th transformer and k-th DG at period t.
$O^{LN}_{kr,t}, O^{ST}_{k,t}$ $O^{TR}_{kr,t}, O^{DG}_{k,t}$	Binary variables representing the accumulation of binary variables $x^{LN}_{kr,t}, x^{ST}_{k,t}, x^{TR}_{kr,t}, x^{DG}_{k,t}$ from 1 to t.
$P_{kr,t}, Q_{kr,t}$	Active and reactive power flows on (k, r)-th transmission line and transformer at period t.
$P^{ST}_{k,t}, P^{DG}_{k,t}, Q^{ST}_{k,t}, Q^{DG}_{k,t}$	Active and reactive power outputs by k-th substations and DG at period t.
$W_{ij,t}$	Power flow on line ij at period t in the fictitious network.
$W^{ST}_{k,t}, W^{LD}_{k,t}$	Generation and load at bus k at period t in the fictitious network.
$U_{k,t}$	Squared voltage magnitude at bus k at period t.
$I_{kr,t}$	Squared branch current on the line (k, r) at period t.
$\alpha_{kr,t,v}, \beta_{kr,t,v}$ $\alpha_{k,t,v}, \beta_{k,t,v}$	Dummy variables for linearizing capacity constraints of line flows and DGs.

I. Introduction

According to the US Energy Information Administration (EIA) in *International Energy Outlook 2016* [1], [2], the share of total renewable energy production will expand from 22% in 2012 to 29% in 2040. China also has been actively promoting the growth of renewable energy resources (RERs) through several initiatives such as the *Action Plan of Energy Development Strategy* issued by the state council. Among various RERs, Distributed Generators (DGs), which are flexible and easy to install, are growing rapidly globally. It is expected that DGs will play an increasingly important role in reshaping the future of electric power systems. DGs often represent small, stand-alone power generation systems which are less than 10 MW and installed in distribution networks near load centers to defer long-distance power transmission lines.

RERs possess a low energy-density requiring an enormous space for large-scale and often costly installations of wind or solar power plant. An alternative is to develop DGs which could be scattered in distribution systems with significant impacts on large thermal power supply, transmission network, and retail consumers [3]. The integration of DGs at high penetration levels could have an effect on the economics and the reliability of distribution networks. Thus, the distribution network planning with DGs, known as the active distribution network planning (ADNP), commands additional studies on power system cost-benefit analyses with a special attention to the impact of ADNP on power system operation and control.

ADNP is a mixed-integer nonlinear programming problem which can be modeled as either static or dynamic system [4], [5]. In a static formulation, the ADNP problem is solved at a single period and investment decisions are made at the beginning of the planning period [6], [7]. In a dynamic formulation, network investments are determined over several successive planning periods according to the practical requirements of each period [8], [9]. The dynamic approach is flexible, but suffers from large dimensionality and faces difficulties in formulating and solving the problem considering the linkage between periods.

In terms of solution, several numerical methods were widely applied to the multi-period ADNP problem. Reference [10] presented a spatial power network planning problem which considers environmental factors in electric line routing. A joint extension planning model of multi-period DGs and distribution networks was proposed in [11] and [12] without considering DG uncertainties. Reference [13] investigated the incorporation of DG investment decisions in a multi-period distribution expansion planning problem considering the timing, location, and sizing of DG units. Reference [14] proposed a multi-period long-term expansion planning model which was linearized to form a mixed-integer linear programming (MILP) model which was solved by classical optimization tools. In [15], an integrated model was set up by taking into account the load growth uncertainty and multi-period and multi-objective optimal ADNP. Reference [16] presented an ADNP model considering medium- and low-voltage systems for minimizing investment, operation, and reliability costs. In [17], a multi-period ADNP model was proposed with a piecewise linear objective function and reliability constraints.

Reference [18] presented a new model for considering DGs in an ADNP, in which the optimal power flow (OPF) was proposed to minimize capital costs for network upgrades, operation and maintenance costs, where a modified genetic algorithm was used to find the optimal solution. Reference [19] proposed a mixed-integer conic programming formulation for the minimum loss distribution network reconfiguration problem. Reference [20] set up a model to incorporate both uncertainty and reliability in the dynamic expansion planning of distribution network with DGs, and proposed an iterative algorithm to yield a pool of high-quality candidate solutions. In [21], a new multistage distribution expansion planning model was proposed to minimize investments on distribution network, which included DG, energy storage, and electric vehicle charging stations.

Reference [22] introduced a mixed-integer conic relaxation technique to handle long-term distribution system expansion planning. In [23] and [24], a two-stage robust optimization was proposed for active distribution networks to address the impact of uncertain DGs and a column-and-constraint generation method was designed. Reference [25] reported a new model to reformulate the microgrid problem in resilient distribution networks, in which the number of binary and continuous variables was significantly reduced and the computational performance was improved. In the early literature, heuristic methods were developed to deal with a nonconvex ADNP problem. References [26]–[28] applied the improved Genetic Algorithm (GA) to the multi-period, multi-level and multi-objective ADNP planning model.

Reference [29] proposed an ADNP model based on GA in which the DG access and load uncertainty were considered. Reference [30] deployed data envelopment analyses along with GA to solve multi-period ADNP in which a load location was considered as a variable. Considering the use of nonconvex distribution power flow equations in a complex ADNP, a decomposed ADNP optimization model with multiple subproblems was proposed. In [21], the first subproblem was responsible for identifying maximum stress conditions in each ADNP period. The second subproblem defined the installation period in network investments. Additionally, the improved Tabu Search was proposed to solve a large-scale ADNP problem [32] and [33]. Reference [34] proposed a multi-objective TSA to solve the multi-period ADNP problem in which the system reliability was evaluated.

To address the stochastic nature of DGs in distribution networks, a restricted operation scenario selection method was proposed in [35] and implemented in the multi-period bi-level ADNP model. To reduce the computational complexity, a selection technique was used based on shadow prices. Furthermore, a multi-objective and multi-level oriented ADNP model was set up in [36] to accommodate high-penetrated RESs, where a *K*-means-cluster based multi-scenarios tool was employed to address uncertainties. Then, a two-stage robust optimization model was set up in [37] to deal with a dynamic reconfiguration problem considering load and DG uncertainties. References [38] and [39] developed a two-stage multi-period stochastic planning model where load and renewable energy uncertainties were considered. Similarly, a large-scale mixed-integer program was presented as a two-stage stochastic programming model for optimal DG locations [40].

The previous papers for the multi-period ADNP utilized a two-stage stochastic programming model, in which planning decisions were made before the realization of uncertainties and could not be adjusted in a multi-period horizon. In order to generate more flexible planning decisions that address uncertainties, this paper proposes a multi-stage stochastic programing in a multi-period ADNP optimization model with DG uncertainties. The main contributions are presented as:

1) A multi-stage stochastic programming approach is proposed for the multi-period ADNP to address DG uncertainties over planning periods. The proposed model, which outperforms a traditional two-stage stochastic programming approach, is equivalent to a dynamic programming reformulation in which the planning decisions are sequentially made with the realization of uncertainties.
2) A stochastic nested decomposition method, referred to as stochastic dual dynamic integer programming (SDDIP), is introduced to decompose the large-scale optimization model and reduce the computational complexity of the proposed large-scale multi-stage stochastic programming model.

The paper is organized as follows: in Section II, a deterministic ADNP model with DGs is set up. Section III designs a nested decomposition by SDDIP for the proposed ADNP model to address uncertainties. Here, forward and backward passes are conducted iteratively with strengthened Benders cuts. In Section IV, numerical results are provided and analyzed. Section V draws the main conclusions.

II. Deterministic ADNP Model With DGs

In this paper, the ADNP model is conducted by a distribution company for investing on the distribution equipment, including lines, substations, transformers, and DGs, to satisfy load requirements. Intuitively, additional investments on DGs could reduce the respective substations costs. Therefore, the two planning alternatives should be traded off.

A. Objective Function

For the proposed ADNP model, the objective is to minimize the total investment and operation costs. The net present value (NPV) of the ADNP objective is expressed as

$$\min \quad \sum_{t=1}^{T} (1+\sigma)^{-t} \left(C_t^{inv} + C_t^{oper}\right) \tag{1}$$

where C_t^{inv} and C_t^{oper} are investment and operation costs at period *t*, respectively.

1) Investment Cost: We consider the investment on four types of assets including lines, substations, transformers and DGs. The total investment cost of each equipment will be transformed into annual investment cost based on the equipment lifetime [18]. Considering equipment lifetimes, the investment cost in the proposed model can be formulated as

$$\begin{aligned} C_t^{inv} = & \sum_{(k,r)\in\Omega^{LN}} \frac{\sigma\delta_{kr,t}^{LN} x_{kr,t}^{LN}}{1-(1+\sigma)^{-\chi_{kr}^{LN}}} + \sum_{k\in\Omega^{ST}} \frac{\sigma\delta_{k,t}^{ST} x_{k,t}^{ST}}{1-(1+\sigma)^{-\chi_{k}^{ST}}} \\ & + \sum_{(k,r)\in\Omega^{TR}} \frac{\sigma\delta_{kr,t}^{TR} x_{kr,t}^{TR}}{1-(1+\sigma)^{-\chi_{kr}^{TR}}} + \sum_{k\in\Omega^{DG}} \frac{\sigma\delta_{k,t}^{DG} x_{k,t}^{DG}}{1-(1+\sigma)^{-\chi_{k}^{DG}}} \end{aligned} \tag{2}$$

2) Operation Cost: The operation cost includes maintenance and power purchase costs. The distribution network maintenance cost is expressed as

$$\begin{aligned} C_t^{M} = & \sum_{(k,r)\in\Omega^{LN}} \gamma_{kr,t}^{LN} y_{kr,t}^{LN} + \sum_{k\in\Omega^{ST}} \gamma_{k,t}^{ST} y_{k,t}^{ST} \\ & + \sum_{(k,r)\in\Omega^{TR}} \gamma_{kr,t}^{TR} y_{kr,t}^{TR} + \sum_{k\in\Omega^{DG}} \gamma_{k,t}^{DG} y_{k,t}^{DG} \end{aligned} \tag{3}$$

The power purchase cost is expressed as

$$C_t^{E} = \lambda_t^{ST} \sum_{k\in\Omega^{ST}} P_{k,t}^{ST} \tag{4}$$

The total operation cost C_t^{oper} is expressed as

$$C_t^{oper} = C_t^{M} + C_t^{E} \tag{5}$$

B. Constraints

The ADNP constraints include those of power flow, network topology requirements, and logical constraints.

1) Power Flow Constraints: The ADNP solution would maintain power and voltage magnitudes within permissible ranges shown in (6)–(19). We use the square of voltage magnitude $U_{k,t}$ and branch current $I_{kr,t}$. Specifically, (6) defines the square of nodal voltage limits and (7) specifies the square of substation voltage magnitude

$$\left(U_k^{\min}\right)^2 \le U_{k,t} \le (U_k^{\max})^2, \ \ \forall k \in \Omega^N, t = 1, \dots, T \quad (6)$$

$$U_{k,t} = \left(U_k^0\right)^2, \ \ \forall k \in \Omega^{ST}, t = 1, \dots, T \quad (7)$$

Constraint (8) specifies the square of branch current limits for lines and transformers. If a line or a transformer is on outage, there is no current flow.

$$0 \le I_{kr,t} \le y_{kr,t}^{LN}\left(I_{kr}^{LN,\max}\right)^2, \ \ \forall (k,r) \in \Omega^{LN}, t = 1, \dots, T \quad (8a)$$

$$0 \le I_{kr,t} \le y_{kr,t}^{TR}\left(I_{kr}^{TR,\max}\right)^2, \ \ \forall (k,r) \in \Omega^{TR}, t = 1, \dots, T \quad (8b)$$

Constraint (9) specifies active and reactive power flows for lines and transformers. If a line or transformer is on outage, the respective active and reactive powers will be zero.

$$\sqrt{P_{kr,t}^2 + Q_{kr,t}^2} \le y_{kr,t}^{LN} S_{kr}^{LN,\max}, \ \forall (k,r) \in \Omega^{LN}, t = 1, \dots, T \quad (9a)$$

$$\sqrt{P_{kr,t}^2 + Q_{kr,t}^2} \le y_{kr,t}^{TR} S_{kr}^{TR,\max}, \ \forall (k,r) \in \Omega^{TR}, t = 1, \dots, T \quad (9b)$$

Constraints (10)–(13) are substation and DG capacity limits. Likewise, if a substation or DG is not operational, the corresponding power is zero.

$$0 \le P_{k,t}^{ST} \le y_{k,t}^{ST} P_k^{ST,\max}, \ \ \forall k \in \Omega^{ST}, t = 1, \dots, T \quad (10)$$

$$0 \le Q_{k,t}^{ST} \le y_{k,t}^{ST} Q_k^{ST,\max}, \ \ \forall k \in \Omega^{ST}, t = 1, \dots, T \quad (11)$$

$$0 \le P_{k,t}^{DG} \le y_{k,t}^{DG} P_k^{DG,\max}, \ \ \forall k \in \Omega^{DG}, t = 1, \dots, T \quad (12)$$

$$\sqrt{\left(P_{k,t}^{DG}\right)^2 + \left(Q_{k,t}^{DG}\right)^2} \le y_{k,t}^{DG} S_k^{DG,\max}, \forall k \in \Omega^{DG}, t = 1, \dots, T \quad (13)$$

Finally, (14) restricts the DG penetration capacity to maintain the distribution system safety.

$$\sum_{k \in \Omega^{DG}} P_{k,t}^{DG} \le \mu \sum_{k \in \Omega^{ST}} P_{k,t}^{ST}, \quad t = 1, \dots, T \quad (14)$$

The precise line flow model [19] is utilized to characterize the distribution power balance and voltage drop,

$$\begin{cases} \sum\limits_{(k,i) \in \Omega^B} P_{ki,t} - \sum\limits_{(j,k) \in \Omega^B} P_{jk,t} = P_{k,t}^{DG} + P_{k,t}^{ST} - P_{k,t}^{LD} \\ \sum\limits_{(k,i) \in \Omega^B} Q_{ki,t} - \sum\limits_{(j,k) \in \Omega^B} Q_{jk,t} = Q_{k,t}^{DG} + Q_{k,t}^{ST} - Q_{k,t}^{LD} \end{cases},$$
$$\forall k \in \Omega^N, t = 1, \dots, T \quad (15)$$

$$-M\left(1 - y_{kr,t}^{LN}\right) \le U_{k,t} - U_{r,t} - 2\left(R_{kr} P_{kr,t} + X_{kr} Q_{kr,t}\right) + \left(R_{kr}^2 + X_{kr}^2\right) I_{kr,t} \le M\left(1 - y_{kr,t}^{LN}\right),$$
$$\forall (k,r) \in \Omega^{LN}, t = 1, \dots, T \quad (16a)$$

$$-M\left(1 - y_{kr,t}^{TR}\right) \le U_{k,t} - U_{r,t} - 2\left(R_{kr} P_{kr,t} + X_{kr} Q_{kr,t}\right) + \left(R_{kr}^2 + X_{kr}^2\right) I_{kr,t} \le M\left(1 - y_{kr,t}^{TR}\right),$$
$$\forall (k,r) \in \Omega^{TR}, t = 1, \dots, T \quad (16b)$$

However, (9a), (9b) and (13) are convex with second-order cone (SOC) nonlinear constraints, which can be tightly linearized [19]. For a general SOC constraint, $\sqrt{z_1^2 + z_2^2} \le z_3$, we consider N_v segments to linearize the SOC constraint with dummy variables $(\alpha_0, \dots, \alpha_{N_v})$ and $(\beta_0, \dots, \beta_{N_v})$, such that

$$\begin{cases} -\alpha_0 \le z_1 \le \alpha_0 \\ -\beta_0 \le z_2 \le \beta_0 \\ \alpha_v = \cos\left(\frac{\pi}{2^{v+1}}\right)\alpha_{v-1} + \sin\left(\frac{\pi}{2^{v+1}}\right)\beta_{v-1} \\ -\beta_v \le -\sin\left(\frac{\pi}{2^{v+1}}\right)\alpha_{v-1} \\ \qquad + \cos\left(\frac{\pi}{2^{v+1}}\right)\beta_{v-1} \le \beta_v \\ \alpha_{N_v} \le z_3 \\ \beta_{N_v} \le \tan\left(\frac{\pi}{2^{N_v+1}}\right)\alpha_{N_v} \end{cases}, v = 1, \dots, N_v \quad (17)$$

Furthermore, (9a), (9b) and (13) are linearized by the following constraints

$$\begin{cases} -\alpha_{kr,t,0} \le P_{kr,t} \le \alpha_{kr,t,0} \\ -\beta_{kr,t,0} \le Q_{kr,t} \le \beta_{kr,t,0} \\ \alpha_{kr,t,v} = \cos\left(\frac{\pi}{2^{v+1}}\right)\alpha_{kr,t,v-1} + \sin\left(\frac{\pi}{2^{v+1}}\right)\beta_{kr,t,v-1} \\ -\beta_{kr,t,v} \le -\sin\left(\frac{\pi}{2^{v+1}}\right)\alpha_{v-1} \\ \qquad + \cos\left(\frac{\pi}{2^{v+1}}\right)\beta_{kr,t,v-1} \le \beta_{kr,t,v} \\ \alpha_{kr,t,N_v} \le y_{kr,t}^{LN} S_{kr}^{LN,\max} \\ \beta_{kr,t,N_v} \le \tan\left(\frac{\pi}{2^{N_v+1}}\right)\alpha_{kr,t,N_v} \end{cases},$$
$$\forall (k,r) \in \Omega^{LN}, t = 1, \dots, T, v = 1, \dots, N_v \quad (18a)$$

$$\begin{cases} -\alpha_{kr,t,0} \le P_{kr,t} \le \alpha_{kr,t,0} \\ -\beta_{kr,t,0} \le Q_{kr,t} \le \beta_{kr,t,0} \\ \alpha_{kr,t,v} = \cos\left(\frac{\pi}{2^{v+1}}\right)\alpha_{kr,t,v-1} + \sin\left(\frac{\pi}{2^{v+1}}\right)\beta_{kr,t,v-1} \\ -\beta_{kr,t,v} \le -\sin\left(\frac{\pi}{2^{v+1}}\right)\alpha_{v-1} \\ \qquad + \cos\left(\frac{\pi}{2^{v+1}}\right)\beta_{kr,t,v-1} \le \beta_{kr,t,v} \\ \alpha_{kr,t,N_v} \le y_{kr,t}^{TR} S_{kr}^{TR,\max} \\ \beta_{kr,t,N_v} \le \tan\left(\frac{\pi}{2^{N_v+1}}\right)\alpha_{kr,t,N_v} \end{cases},$$
$$\forall (k,r) \in \Omega^{TR}, t = 1, \dots, T, v = 1, \dots, N_v \quad (18b)$$

$$\begin{cases} -\alpha_{k,t,0} \le P_{k,t}^{DG} \le \alpha_{k,t,0} \\ -\beta_{k,t,0} \le Q_{k,t}^{DG} \le \beta_{k,t,0} \\ \alpha_{k,t,v} = \cos\left(\frac{\pi}{2^{v+1}}\right)\alpha_{k,t,v-1} + \sin\left(\frac{\pi}{2^{v+1}}\right)\beta_{k,t,v-1} \\ -\beta_{k,t,v} \le -\sin\left(\frac{\pi}{2^{v+1}}\right)\alpha_{v-1} + \cos\left(\frac{\pi}{2^{v+1}}\right)\beta_{k,t,v-1} \le \beta_{k,t,v} \\ \alpha_{k,t,N_v} \le y_{k,t}^{TR} S_k^{DG,\max} \\ \beta_{k,t,N_v} \le \tan\left(\frac{\pi}{2^{N_v+1}}\right)\alpha_{k,t,N_v} \end{cases},$$
$$\forall (k,r) \in \Omega^{DG}, t = 1, \dots, T, v = 1, \dots, N_v \quad (18c)$$

Fig. 1. 6-bus Network diagram.

2) Network Topology Constraints: During investment and operation periods, the distribution network can be reconfigured to achieve the optimal operation. However, the radial property and the connectivity should be strictly preserved. According to the necessary condition stated by the graph theory [41]–[44], the total number of lines in a radial network is equal to the total number of buses minus the number of roots (i.e., substations), so

$$\sum_{(k,r)\in\Omega^{LN}} y_{kr,t}^{LN} + \sum_{(k,r)\in\Omega^{TR}} y_{kr,t}^{TR} = N^b - \sum_{k\in\Omega^{ST}} y_{k,t}^{ST}, t=1,\ldots,T \tag{19}$$

However, (19) cannot sufficiently guarantee the radiality of distribution network. For example, Fig. 1 depicts a 6-node system, where bus 3 is an isolated node and there is a loop. The topology in Fig. 1 satisfies (19), but the distribution network is not a connected network.

To address the problem, we consider a fictitious network where all nodes have loads except for the substation. Fictitious network is a network has the same topology as that of the physical network but has different net loads. To realize the idea, the flow decision variables for physical and fictitious networks are different while the topology decision variables are the same. If all nodes in the fictitious network can satisfy power flow conditions, the connectivity of all nodes will be guaranteed. The power flow equations in the fictitious network will only constrain the connectivity of buses, so the equations are simplified as

$$\sum_{(i,k)\in\Omega^B} W_{ik,t} - \sum_{(k,j)\in\Omega^B} W_{kj,t} = W_{k,t}^{ST} - W_{k,t}^{LD}, \tag{20}$$

$$\forall k \in \Omega^N, t=1,\ldots,T$$

$$-y_{kr,t}^{LN}M \le W_{kr,t} \le y_{kr,t}^{LN}M,\ \forall (k,r)\in\Omega^{LN}, t=1,\ldots,T \tag{21}$$

$$-y_{k,t}^{ST}M \le W_{k,t}^{ST} \le y_{k,t}^{ST}M \quad \forall k\in\Omega^{ST}, t=1,\ldots,T \tag{22}$$

$$W_{k,t}^{LD} = 1, \quad \forall k \in \Omega^{LD}, t=1,\ldots,T \tag{23}$$

where (20) specifies the power balance at each mode in the fictitious network; (21) and (22) indicate that the power flow should be zero if the line or substation is not constructed; (23) shows that the load demand at each node in the fictitious network is specified as 1 unit. Constraints (20)–(23) refer to the commodity flow. If (20)–(23) are satisfied, there is at least one path that connects the sink with each node, suggesting that the network must be connected. It is noted that the original power flow constraint (15) cannot fully guarantee the network connectivity because some nodes might have a zero power injection. If all the nodes have nonzero power injection, (20)–(23) are redundant and can be eliminated.

3) Logical Constraints: First, the investment on each equipment is done only once, which is expressed as

$$\sum_{t=1}^{T} x_{kr,t}^{LN} \le 1, \forall (k,r)\in\Omega^{LN},$$

$$\sum_{t=1}^{T} x_{k,t}^{ST} \le 1, \forall k\in\Omega^{ST} \tag{24}$$

$$\sum_{t=1}^{T} x_{kr,t}^{TR} \le 1, \forall (k,r)\in\Omega^{TR},$$

$$\sum_{t=1}^{T} x_{k,t}^{DG} \le 1, \forall k\in\Omega^{DG} \tag{25}$$

Second, binary variables representing the network topology $(y_{kr,t}^{LN}, y_{kr,t}^{TR})$ are coupled with investment decision variables. However, an equipment is put into operation once it is planned, i.e., $(y_{kr,t}^{LN}, y_{kr,t}^{TR}) = 1$. This condition gives way to the following constraints,

$$y_{kr,t}^{LN} \le \sum_{h=1}^{t} x_{kr,h}^{LN}, \quad \forall (k,r)\in\Omega^{LN}, t=1,\ldots,T \tag{26}$$

$$y_{k,t}^{ST} \le \sum_{h=1}^{t} x_{k,h}^{ST}, \quad \forall k\in\Omega^{ST}, t=1,\ldots,T \tag{27}$$

$$y_{kr,t}^{TR} \le \sum_{h=1}^{t} x_{kr,h}^{TR}, \quad \forall (k,r)\in\Omega^{TR}, t=1,\ldots,T \tag{28}$$

$$y_{k,t}^{DG} \le \sum_{h=1}^{t} x_{k,h}^{DG}, \quad \forall k\in\Omega^{DG}, t=1,\ldots,T \tag{29}$$

Moreover, a transformer is added only after its substation is planned. This constraint is expressed as

$$x_{kr,t}^{TR} \le \sum_{h=1}^{t} x_{k,h}^{ST}, y_{kr,t}^{TR} \le y_{k,t}^{ST}, \quad \forall k\in\Omega^{ST}, t=1,\ldots,T \tag{30}$$

However, temporal constraints (24)–(30) linking more than two periods are equivalent to those in dynamic programming reformulation in which the decision at period t would only depend on that of the previoius period. Define

$$O_{kr,t}^{LN} = \sum_{h=1}^{t} x_{kr,h}^{LN}, O_{k,t}^{ST} = \sum_{h=1}^{t} x_{k,h}^{ST}, O_{kr,t}^{TR} = \sum_{h=1}^{t} x_{kr,h}^{TR}, O_{k,t}^{DG} = \sum_{h=1}^{t} x_{k,h}^{DG}$$

$$, t=1,\ldots,T \tag{31}$$

Constraints (24)-(30) are exactly reformulated as

$$\begin{aligned}&O_{kr,T}^{LN} \leq 1, \forall (k,r) \in \Omega^{LN}, O_{k,T}^{ST} \leq 1, \forall k \in \Omega^{ST}\\&O_{kr,T}^{TR} \leq 1, \forall (k,r) \in \Omega^{TR}, O_{k,T}^{DG} = 1, \forall k \in \Omega^{DG}\\&t = 1, \ldots, T\end{aligned} \tag{32}$$

$$\begin{aligned}&y_{kr,t}^{LN} \leq \delta_{kr,t}^{LN}, \forall (k,r) \in \Omega^{LN}, y_{k,t}^{ST} \leq \delta_{k,t}^{ST}, \forall k \in \Omega^{ST}\\&y_{kr,t}^{TR} \leq \delta_{kr,t}^{TR}, \forall (k,r) \in \Omega^{TR}, y_{k,t}^{DG} \leq \delta_{k,t}^{DG}, \forall k \in \Omega^{DG}\\&, t = 1, \ldots, T\end{aligned} \tag{33}$$

$$\begin{aligned}&O_{kr,t}^{LN} = O_{kr,t-1}^{LN} + x_{kr,t}^{LN}, \forall (k,r) \in \Omega^{LN},\\&O_{k,t}^{ST} = O_{k,t-1}^{ST} + x_{k,t}^{ST}, \forall k \in \Omega^{ST}\\&O_{kr,t}^{TR} = O_{kr,t-1}^{TR} + x_{kr,t}^{TR}, \forall (k,r) \in \Omega^{TR},\\&O_{k,t}^{DG} = O_{k,t-1}^{DG} + x_{k,t}^{DG}, \forall k \in \Omega^{DG}\\&, t = 1, \ldots, T\end{aligned} \tag{34}$$

$$x_{kr,t}^{TR} \leq x_{k,h}^{ST}, y_{kr,t}^{TR} \leq y_{k,t}^{ST}, \quad \forall k \in \Omega^{ST}, t = 1, \ldots, T \tag{35}$$

For the above planning model, define $\boldsymbol{z}_t$ and $\boldsymbol{q}_t$ as the sets of binary and continuous decision variables, respectively. Constraints (2)–(23) are only related to the decision variables $(\boldsymbol{z}_t, \boldsymbol{q}_t)$ at each period, and (32)–(35) linking two consecutive periods are only associated with binary variables (i.e., planning decisions $\boldsymbol{x}_t$). Moreover, the current value of z_0 is deterministic. Therefore, the optimization model (1) subject to (2)–(23) and (32)–(35) is mathematically stated as

$$\min_{\boldsymbol{z}_t, \boldsymbol{q}_t} \sum_{t=1}^{T} \left(\boldsymbol{c}_t^T \boldsymbol{z}_t + \boldsymbol{d}_t^T \boldsymbol{q}_t \right) \tag{36a}$$

$$\text{s.t. } \boldsymbol{B}_t \boldsymbol{z}_{t-1} + \boldsymbol{A}_t \boldsymbol{z}_t \geq \boldsymbol{b}_t, \ t = 1, \ldots, T \tag{36b}$$

$$\boldsymbol{z}_t \in \{0,1\}, \ \ (\boldsymbol{z}_t, \boldsymbol{q}_t) \in \Omega_t, \ \ t = 1, \ldots, T \tag{36c}$$

III. Nested Decomposition by SDDIP for Multi-Stage Stochastic Programming of ADNP

The optimization model (36) is stated for a specific net load (i.e., load demand minus DG output). In this paper, we consider that all DGs are renewable with variable generation outputs. Thus, the corresponding net load uncertainty will affect planning decisions. This paper proposes a stochastic programming model with multiple scenarios for calculating the uncertain decision variables.

At first, we apply a scenario tree to characterize the uncertainties and describe possible sequential realizations as depicted in Fig. 2. Let $(\xi_1^s, \xi_2^s, \ldots, \xi_T^s)$ denote the s-th scenario with each ξ_t^srepresenting a realization of the s-th scenario at the period t. We consider that each scenario $(\xi_1^s, \xi_2^s, \ldots, \xi_T^s)$ is stage-wise independent (i.e., Markovian). The detailed modeling for a scenario tree can be found in [45].

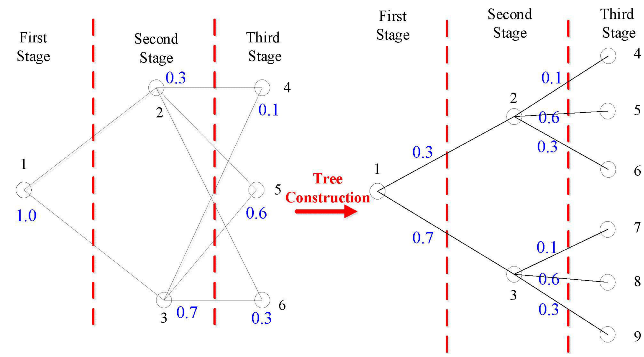

Fig. 2. A scenario tree.

Since the distribution planning problem is essentially a multi-period optimization problem, the decisions should be made sequentially with respect to the gradual realization of the random process for uncertainties $\xi_1,\ldots,\xi_T$, where ξ_t denotes the uncertainty at period t. From the distribution planning model (33), the uncertainties only exist in Ω_t, i.e., $\Omega_t(\xi_t)$. This gives a multi-stage stochastic programming (MSSP) as shown in (37) shown at the bottom of this page, [46], where the feasible region is expressed as

$$\begin{aligned}&\chi_t\left(\boldsymbol{z}_{t-1}, \xi_t\right) = \{\boldsymbol{z}_t \in \{0,1\} \,|\boldsymbol{A}_t \boldsymbol{z}_t\\&\geq \boldsymbol{b} - \boldsymbol{B}_t \boldsymbol{z}_{t-1,t}, (\boldsymbol{z}_t, \boldsymbol{q}_t) \in \Omega_t\left(\xi_t\right)\}\\&t = 1, \ldots, T,\end{aligned} \tag{38}$$

The multi-stage optimization model indicates that the planning decisions $z_1,\ldots,\ z_T$ should be flexible to the random process, which have the form as: Observation $(\xi_1)\rightarrow$ Decision $\{z_1(\xi_1)\}$ $\rightarrow$ Observation $(\xi_1,\ \xi_2)$ $\rightarrow$ Decision $\{z_2(\xi_1,\ \xi_2)\}$ $\rightarrow\cdots\rightarrow$ Observation $(\xi_1, \xi_2,\ldots, \xi_T)\rightarrow$ Decision $\{z_T(\xi_1, \xi_2,\ldots, \xi_T)\}$. This implies that the decision variables $z_t = z_t(\xi_1, \xi_2,\ldots, \xi_t)$ for $t = 1,\ldots,T$ is a function of the random process $(\xi_1, \xi_2,\ldots, \xi_t)$ up to time t. This is called a *policy*. The MSSP can be cast as a nested mixed integer stochastic formulation [47]–[52]. To handle this problem, we present a nested decomposition by SDDIP. The main idea includes four steps: (i) stop criteria; (ii) random sampling, (iii) forward pass, and (iv) backward pass. The detailed flowchart is shown in Table I.

Specifically, we state the following:

i) The stopping criterion can be chosen by estimating the optimal gap. Let μ and σ represent the mean and the variance of the objective value for N samples. The lower bound is the objective value from any relaxed optimization model. Usually, we can choose the optimal objective value of a single-stage problem at the first stage as the lower bound. The upper bound is a confidence interval $[\mu - z_{\alpha/2}\frac{\sigma}{\sqrt{N}}, \mu + z_{\alpha/2}\frac{\sigma}{\sqrt{N}}]$, where $z_{\alpha/2}$ is the 1-α quantile of the standard normal distribution. Intuitively, the

$$\min_{(\boldsymbol{z}_1,\boldsymbol{q}_1)\in\chi_1(\boldsymbol{z}_0,\xi_1)} \boldsymbol{c}_1^T\boldsymbol{z}_1 + \boldsymbol{d}_1^T\boldsymbol{q}_1 + \mathbb{E}\left[\inf_{(\boldsymbol{z}_2,\boldsymbol{q}_2)\in\chi_2(\boldsymbol{z}_1,\xi_2)} \boldsymbol{c}_2^T\boldsymbol{z}_2 + \boldsymbol{d}_1^T\boldsymbol{q}_1 + \mathbb{E}\left[\ldots + \mathbb{E}\left[\inf_{(\boldsymbol{z}_T,\boldsymbol{q}_T)\in\chi_T(\boldsymbol{z}_{T-1},\xi_T)} \boldsymbol{c}_T^T\boldsymbol{z}_T + \boldsymbol{d}_T^T\boldsymbol{q}_T\right]\right]\right] \tag{37}$$

TABLE I
FLOWCHART OF NESTED SDDIP DECOMPOSITION

Nested Decomposition by SDDIP
Initialize $LB \leftarrow -\infty$, $UB \leftarrow +\infty$ and $i \leftarrow 1$
while the stopping criterion (35) is satisfied
Sample N scenarios $\xi^s = (\xi_1^s, \xi_2^s, \ldots, \xi_T^s)$, $s=1,\ldots,N$;
for $s=1,\ldots,N$
for $t=1,\ldots,T$
Solve the model (36) and obtain $\left(\overline{z}_{t,s}^{i}, \overline{q}_{t,s}^{i}\right)$;
end
$\tau_s^i \leftarrow \sum_{t=1}^{T} c_t^T \overline{z}_{t,s}^{i} + d_t^T \overline{q}_{t,s}^{i}$;
end
$\mu^i \leftarrow \frac{1}{N}\sum_{s=1}^{N} \tau_s^i$ and $\sigma^i \leftarrow \sqrt{\frac{1}{N-1}\sum_{s=1}^{N}\left(\tau_s^i - \mu^i\right)^2}$;
$UB \leftarrow \mu^i + z_\alpha \frac{\sigma^i}{\sqrt{N}}$;
for $t=T,\ldots,2$
for $s=1,\ldots,N$
for $j=1,\ldots,N_t$
Solve (38)-(39) to get ρ_{ts}^i and $\overline{Z}_{ts}^i$;
end
Generate a cut by (38) and add it into the mode (36);
end
end
Solve (35) by $Q_1^i\left(z_0^i, \xi_1\right)$ and $LB \leftarrow c_1^T \overline{z}_1^i + d_1^T \overline{q}_1^i$; $i \leftarrow i+1$;
end

algorithm can be stopped if the gap between lower and upper bounds is small enough. Since any value within the confidence interval can be served as the upper bound, we will choose the supremum of the confidence interval as the upper bound to guarantee the optimality, which gives

$$UB - LB \leq \varepsilon, UB = \mu + z_{\alpha/2}\sigma \Big/ \sqrt{N} \tag{39}$$

where $\varepsilon > 0$ denotes the optimality gap.

ii) The random sampling generates N scenarios in the scenario tree to approximate the recourse function at each iteration.

iii) The forward pass will solve dynamic equations from $t = 1$ to $t = T$ for each sampled scenario s. In the i-th iteration, we have

$$Q_{ts}^i\left(\boldsymbol{z}_{t-1,s}^i, \xi_t^s\right) = \min_{\substack{\boldsymbol{A}_t \boldsymbol{z}_{ts}^i \geq \boldsymbol{b} - \boldsymbol{B}_t \boldsymbol{r}_{ts}^i, \boldsymbol{r}_{ts}^i = \boldsymbol{z}_{t-1,s}^i \\ \left(\boldsymbol{z}_{ts}^i, \boldsymbol{r}_{ts}^i\right) \in \{0,1\}, \left(\boldsymbol{z}_{ts}^i, \boldsymbol{q}_{ts}^i, \boldsymbol{r}_{ts}^i\right) \in \Omega_t(\xi_t^s)}} \boldsymbol{c}_t^T \boldsymbol{z}_{ts}^i + \boldsymbol{d}_t^T \boldsymbol{q}_{ts}^i + \vartheta_{t+1}\left(\boldsymbol{z}_{ts}^i\right) \tag{40}$$

Then, a feasible solution is obtained by $(\overline{\boldsymbol{z}}_{1,s}^i, \ldots, \overline{\boldsymbol{z}}_{T,s}^i)$ and $(\overline{\boldsymbol{q}}_{1,s}^i, \ldots, \overline{\boldsymbol{q}}_{T,s}^i)$. Then, the upper bound can be updated by (39).

iv) The backward pass starts from the last stage $t = T$ to the first stage $t = 1$ for each scenario s, which aims to generate cuts at each period to tighten the lower approximation of the recourse functions. Based on $(\overline{\boldsymbol{z}}_{1,s}^i, \ldots, \overline{\boldsymbol{z}}_{T,s}^i)$ from the forward pass, the Lagrangian cut is obtained by solving the Lagrangian dual problem as

$$Z_{ts}^i\left(\overline{\boldsymbol{z}}_{t-1,s}^i, \xi_t^s\right) = \max_{\boldsymbol{\pi}_{ts}^i} \min_{\substack{\boldsymbol{A}_t \boldsymbol{z}_{ts}^i \geq \boldsymbol{b} - \boldsymbol{B}_t \boldsymbol{r}_{ts}^i, \left(\boldsymbol{z}_{ts}^i, \boldsymbol{r}_{ts}^i\right) \in \{0,1\} \\ \left(\boldsymbol{z}_{ts}^i, \boldsymbol{q}_{ts}^i, \boldsymbol{r}_{ts}^i\right) \in \Omega_t(\xi_t^s)}} \boldsymbol{c}_t^T \boldsymbol{z}_{ts}^i + \boldsymbol{d}_t^T \boldsymbol{q}_{ts}^i + \vartheta_t\left(\boldsymbol{z}_{ts}^i\right) - \left(\boldsymbol{\pi}_{ts}^i\right)^T \left(\boldsymbol{r}_{ts}^i - \overline{\boldsymbol{z}}_{t-1,s}^i\right) \tag{41}$$

Since the outer-level model is unconstrained, we can fix the value by the multipliers from the linear relaxation of the inner model, leading to a strengthened Benders cuts as

$$\vartheta_t\left(\boldsymbol{z}_t\right) \geq \left(\frac{1}{N_t}\sum_{s=1}^{N_t} \rho_{ts}^i\right)^T \boldsymbol{z}_t + \frac{1}{N_t}\sum_{s=1}^{N_t} \overline{Z}_{ts}^i, t = T, \ldots, 2 \tag{42}$$

where ρ_{ts}^i and $\overline{Z}_{ts}^i$ are computed by (43) and (44), respectively.

$$\begin{aligned} L_t^i\left(\boldsymbol{\rho}_{ts}^i\right) &= \min \boldsymbol{c}_t^T \boldsymbol{z}_{ts}^i + \boldsymbol{d}_t^T \boldsymbol{q}_{ts}^i + \vartheta_{t+1}\left(\boldsymbol{z}_{ts}^i\right) \\ \text{s.t. } & \boldsymbol{A}_t \boldsymbol{z}_{ts}^i \geq \boldsymbol{b} - \boldsymbol{B}_t \boldsymbol{r}_{ts}^i, \left(\boldsymbol{z}_{ts}^i, \boldsymbol{q}_{ts}^i, \boldsymbol{r}_{ts}^i\right) \in \Omega_t\left(\xi_t^s\right), \\ & \boldsymbol{r}_{ts}^i = \overline{\boldsymbol{z}}_{t-1,s}^i : \boldsymbol{\rho}_{ts}^i \end{aligned} \tag{43}$$

$$\begin{aligned} \overline{Z}_{ts}^i &= \min \boldsymbol{c}_t^T \boldsymbol{z}_{ts}^i + \boldsymbol{d}_t^T \boldsymbol{q}_{ts}^i + \vartheta_{t+1}\left(\boldsymbol{z}_{ts}^i\right) - \left(\boldsymbol{\pi}_{ts}^i\right)^T \boldsymbol{r}_{ts}^i \\ \text{s.t. } & \boldsymbol{A}_t \boldsymbol{z}_{ts}^i \geq \boldsymbol{b} - \boldsymbol{B}_t \boldsymbol{r}_{ts}^i, \left(\boldsymbol{z}_{ts}^i, \boldsymbol{q}_{ts}^i, \boldsymbol{r}_{ts}^i\right) \in \Omega_t\left(\xi_t^s\right) \end{aligned} \tag{44}$$

Discussion: The traditional stochastic programming for the multi-period ADNP in an uncertain environment is essentially a two-stage problem [37]–[40]. All discrete decision variables are calculated as the first stage variables before the realization of uncertainties. This means that first-stage variables are independent of any future information on uncertainties and are identical in all scenarios. The continuous variables serve as the second stage adjustable variables for uncertainties. For the two models, which include two-stage and multi-stage stochastic programming models, the "stage" and "period" are the same in the latter model but different in the former model. The optimal planning decision from the two-stage model is unchanged with the realization of uncertainties, whereas that from the multi-stage model is sequentially changed with respect to the scenarios of uncertainties. At each stage, the decision for the next stage is unique but decisions for future stages can be adjusted to uncertainties. Therefore, the multi-stage model can yield more flexible decisions than the two-stage model.

IV. CASE STUDY

A 33-bus distribution network depicted in Fig. 3, whose data are available from [53], is considered for the simulation over three periods. In this system, buses 2–32 are load buses, and 1 and 34 are two candidate substations. Additional DG parameters, cost coefficients and prices are provided in Table II. A scenario tree in Fig. 3 is used to represent DG and load uncertainties, where there are three stages and the corresponding probabilities are given in Table III. For the first stage, there is only one scenario to represent the current information, where all decisions will be made from. For the second stage, there are

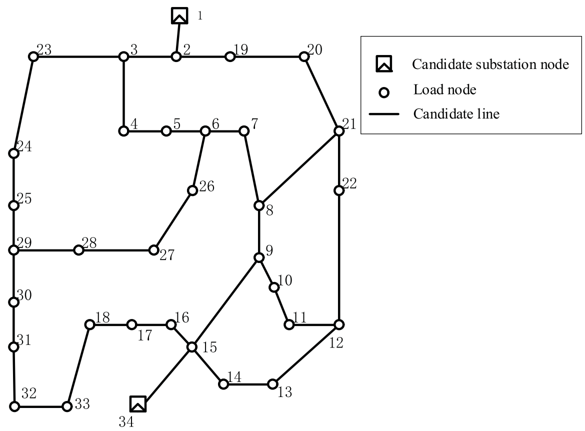

Fig. 3. The candidate 33-bus distribution network.

TABLE II
BASIC PARAMETERS OF THE 33-BUS DISTRIBUTION NETWORK

Parameters	Value
Substation candidate buses	#1 & #33
Load buses	#2 - #32
DG buses	#2 - #32
DG capacity	100kW
Investment cost of lines	200,000 ¥/km
Maintenance cost of lines	20,000 ¥/year
Investment cost of substations	5 million ¥/unit
Maintenance cost of substations	200,000 ¥/year
Investment cost of DGs	200,000 ¥/unit
Maintenance cost of DGs	10,000 ¥/year
Energy price from electricity market	400 ¥/MWh
Annual interest rate	0.03

TABLE III
SCENARIOS FOR UNCERTAIN DG OUTPUT AND LOAD DEMAND

Scenarios	Stages	DG	Load	Probability
1	1	30%	80%	1.0
2	2	70%	80%	0.3
3	2	20%	110%	0.7
4	3	70%	110%	0.1
5	3	40%	120%	0.6
6	3	10%	140%	0.3

two scenarios, representing high and low penetrations of DGs. For the third stage, we set three scenarios, representing high, medium and low penetrations of DGs. Furthermore, two-stage stochastic programming (TSSP), and TSSP with only the load uncertainty (TSWO) are two additional models which are used for comparison with the proposed MSSP. The three models are solved by GUROBI on a computer with quad-core, 2.4 GHz CPU and 4 GB memory. The ADNP solutions for the three distribution network models are shown in Figs. 4–6.

Table IV presents the annual electricity input and minimum voltage profile for the three models. The investment cost (Invest.), annual electricity purchase (Purch.), and maintenance cost (Main.) of the three models are shown in Table V. The investment costs for all three models, occur in the first period.

TABLE IV
TOTAL ELECTRICITY (MWH) AND VOLTAGE LEVELS (P.U.)

Models	Period	Total electricity	Minimum voltage
MSSP	1	9075.36	0.96
	2	8825.40	0.99
	3	20110.59	0.96
	Total	38011.35	-
TSSP	1	9075.36	0.96
	2	9143.06	0.98
	3	25221.13	0.95
	Total	43439.55	-
TSWO	1	9075.36	0.96
	2	15668.03	0.95
	3	50903.62	0.94
	Total	75647.01	-

TABLE V
ADNP COSTS (10^4 ¥)

Models	Period	Invest.	Purch.	Main.	Total
MSSP	1	717.92	352.44	46.60	1116.96
	2	260.83	332.75	63.81	657.39
	3	407.80	736.16	97.41	1241.37
	Total	1386.55	1421.35	207.82	3017.72
TSSP	1	717.92	352.44	46.60	1116.96
	2	296.95	344.73	64.66	706.34
	3	492.79	923.24	103.41	1519.44
	Total	1507.66	1620.41	214.67	3342.74
TSWO	1	717.92	352.44	46.60	1116.96
	2	127.29	590.74	56.18	774.21
	3	620.90	1863.36	95.17	2579.43
	Total	1466.11	2806.54	197.95	4470.60

At the beginning (1st period), the distribution network is constructed for supplying the load buses. This period will result in high investment costs. At the second period, the model with DGs will require an additional investment. However, load cannot be met without the DG support at the third period because the substation capacity is limited. Thus, another substation is planned, which will increase the investment cost of TSWO. Although the installation of DGs will increase the investment cost at the initial stage, the DGs will significantly reduce the total ADNP cost during the next two periods.

Compared with TSSP and TSWO, the proposed MSSP model's reduction in electricity purchase after adding DGs is about 32207.46 MWh in the entire planning period. The total TSSP cost is reduced by 42.27%. In addition, the reverse power flow of DGs will support the distribution network voltage profile, where the minimum voltages in TSSP and MSSP are higher than that of TSWO. In addition, the total MSSP cost is reduced by 10.8% as compared with that of TSSP. Moreover, it can be found that the planning scheme is different under different scenarios, but the decision maker does not obtain the precise prior information. Note that TSSP only produces one planning scheme before the realization of uncertainties, which is similar to TSWO. TSSP finds the ADNP model with the minimum expected cost in which the ADNP solution is fixed for the realization of uncertainties. In contrast, MSSP offers an ADNP decision tree in which the uncertainties are realized as

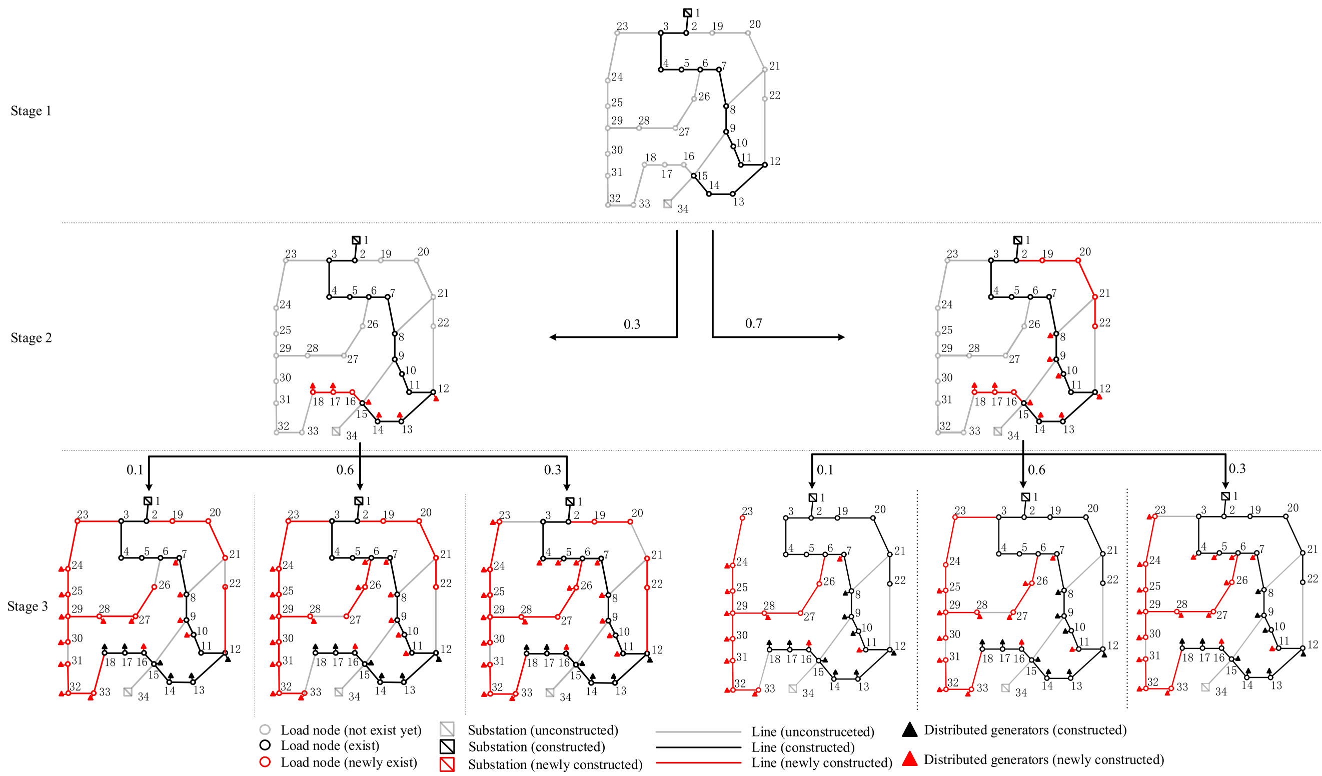

Fig. 4. The planning of the 33-bus distribution system with DGs (MSSP).

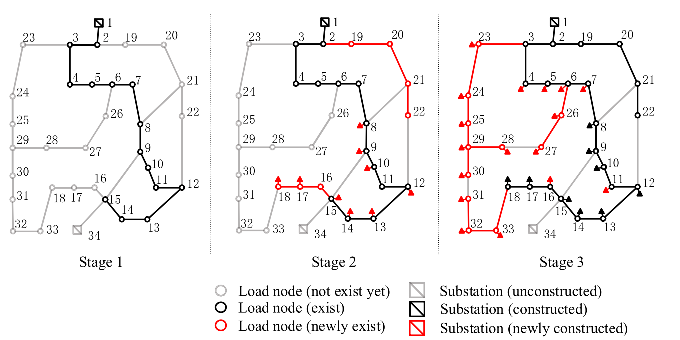

Fig. 5. The planning of the 33-bus distribution system with DGs (TSSP).

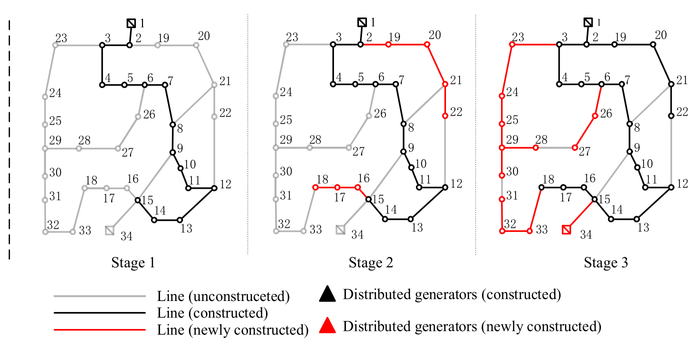

Fig. 6. The planning of the 33-bus distribution system without DGs.

the ADNP solution progresses. Accordingly, the ADNP decision is a wait-and-see scheme which is not completed before the realization of uncertainties.

Using the proposed MSSP solution, there is only one planning decision and several possible future decisions in the first period. In the second period, decision makers wait and see which scenario truly happens and choose the corresponding planning as uncertainties are realized. For example, if the probability of a scenario is 0.3, the remaining planning scheme at the second period will be chosen and the future periods still have multiple possibilities. Once the third period uncertainties are realized, the third period planning will be determined. Therefore, the MSSP decision is more flexible than that of TSSP which can be adjusted according to future period uncertainties. As shown in Table V, the restriction on nodal voltages is in fact loose in the MSSP model, but the restriction is not always loose.

Now, we design four cases to explain this viewpoint on the 33-bus distribution network.

Case 1: The restriction on nodal voltages is removed;

Case 2: The upper bound of voltages is 1.05 p.u., and the lower bound is 0.95 p.u.;

Case 3: The upper bound of voltages is 1.03 p.u., and the lower bound is 0.97 p.u.;

Case 4: The upper bound of voltages is 1.025 p.u. and the lower bound is 0.975 p.u.

The results of the cost and the minimum voltage are shown in Table VI. In both Cases 1 and 2, the minimum voltages during three periods are 0.9729 p.u., 0.9867 p.u. and 0.9676 p.u., and

TABLE VI
TOTAL COST AND VOLTAGE LEVEL IN FOUR CASES

	Period	1	2	3	Total
Case 1	Cost (10^4 ¥)	1116.96	657.39	1241.37	3017.72
	Minimum voltage (p.u.)	0.9729	0.9869	0.9671	-
Case 2	Cost (10^4 ¥)	1116.96	657.39	1241.37	3017.72
	Minimum voltage (p.u.)	0.9729	0.9869	0.9671	-
Case 3	Cost (10^4 ¥)	1116.96	652.71	1251.27	3020.94
	Minimum voltage (p.u.)	0.9729	0.9853	0.9700	-
Case 4	Cost (10^4 ¥)	1140.42	652.71	1261.24	3054.37
	Minimum voltage (p.u.)	0.9751	0.9860	0.9750	-

TABLE VII
SCALABILITY OF THE PROPOSED METHOD

# of Pers	# of Sces	# of BVs	# of CVs	# of Cons	Time (s) T1	Time (s) T2
3	6	3816	5796	10087	61	183
3	27	17172	26082	42028	249	1872
5	6	6360	9660	17131	88	463
5	27	28620	43470	77086	377	>3600
10	6	12720	19320	32341	116	1546
10	27	57240	86940	140091	510	--
20	81	171720	260820	413871	3187	--

the total cost is the lowest at 30.1772 million ¥. This indicates that the voltage magnitudes are not active for these cases. But in Case 3, the minimum voltages during three periods are 0.9729 p.u., 0.9853 p.u. and 0.9700 p.u.; in Case 4, the minimum voltages during three periods are 0.9751 p.u., 0.9919 p.u. and 0.9750 p.u.

This shows that the minimum voltage magnitude reaches the lower bound of the allowable nodal voltages. As a result, the restriction on nodal voltages is tight. Compared with Cases 1 and 2, we conclude that if the lower bound of nodal voltages is below 0.9676 p.u., the voltage restriction will be loose; otherwise, it will be tight. Moreover, we find that increasing the lower bound of voltages will increase the total cost because the feasible region of the optimization model becomes smaller.

In addition, the scalability of the proposed MSSP method is tested for different numbers of periods (# of Pers) and scenarios (# of Sces). Table VII shows that the number of binary variables (# of BVs), continuous variables (# of CVs) and constraints (# of Cons) will increase with increasing the # of Pers and/or Sces, and the computation time will increase accordingly. Moreover, the SDDIP for MSSP (T1) is faster than that of the straightforward method by directly using the CPLEX solver (T2) for 1% gaps. In small-scale cases, i.e., T1 compared with T2 accelerates the speed by 3–10 times. In large-scale cases, T2 fails to solve the proposed MSSP model due to the limited memory space while T1 can still handle the MSSP. Moreover, by increasing either the # of Pers or the # of Sces, T1 will save more time with the help of decomposition and strengthened Benders' cuts.

Finally, we have added a 906-bus distribution network for simulation validation and checking the computation efficiency of the MSSP model for different numbers of periods and scenarios. The data of 906-bus distribution system can be available from [50]. The computation time and the optimal cost are shown in Table VIII. As the numbers of periods and scenarios increase, the computation time will increase from 798s to 5288s accordingly. In particular, the proposed method can efficiently solve the large-scale multi-stage stochastic optimization model within two hours for the case with 5 periods and 40 scenarios, where there are 3278400 continuous variables, 1821600 discrete variables, and 6750028 constraints. Moreover, the optimal cost ranges from 4,000 million ¥ to 5,000 million ¥ for different numbers of periods and scenarios. The increase in the number of periods will reduce the optimal cost because the feasible region of the optimization model becomes larger and there are more choices for decision makers. For the same numbers of time periods, the cost will increase as the number of scenarios increases because some extreme scenarios will result in a higher cost than the expected cost.

TABLE VIII
COMPUTATION TIME AND COST FOR THE 906-BUS DISTRIBUTION SYSTEM

# of Pers	# of Sces	Time (seconds)	Cost (10^6 ¥)
3	6	797.7	4135.17
	8	1033.9	4421.52
	10	1469.1	4961.36
4	12	2314.4	4228.2
	16	2618.9	4399.5
	20	3021.1	4718.8
5	24	3691.2	4289.2
	32	4419.2	4318.4
	40	5287.7	4632.3

V. CONCLUSION

This paper developed a multi-stage stochastic programming for the multi-period ADNP model with uncertain DGs. Compared with a traditional two-stage stochastic programming model which makes the decision simultaneously before the realization of uncertainties, the proposed multi-stage stochastic programming model will give a sequential decision with uncertainties realized at each period. A 33-bus distribution network and a large-scale 906-bus system are tested to show that the multi-stage stochastic approach can provide a better optimal planning scheme than the traditional two-stage stochastic approach. Moreover, the nested SDDIP decomposition method can efficiently solve the proposed model over multiple periods.

REFERENCES

[1] A. C. Santos, C. R. Rio, and D. B. Diez, "Distributed generation: A review of factors that can contribute most to achieve a scenario of DG units embedded in the new distribution networks," *Renew. Sustain. Energy Rev.*, vol. 59, pp. 1130–1148, 2016.

[2] "International energy outlook 2016," US energy information administration, 2016. [Online]. Available: http://www.eia.gov/forecasts/ieo/pdf/0484(2016).pdf

[3] J. Li, C. Zhang, Z. Xu, J. Wang, J. Zhao, and Y. Zhang, "Distributed transactive energy trading framework in distribution networks," *IEEE Trans. Power Syst.*, vol. 33, no. 6, pp. 7215–7227, Nov. 2018.

[4] S. Khator and L. Leung, "Power distribution planning: A review of models and issues," *IEEE Trans. Power Syst.*, vol. 12, no. 3, pp. 1151–1159, Aug. 1997.
[5] H. Falaghi, C. Singh, and M. R. Haghifam, "DG integrated multistage distribution system expansion planning," *Int. J. Elec. Power Energy Syst.*, vol. 33, no. 8, pp. 1489–1497, 2011.
[6] V. F. Martins and C. L. T. Borges, "Active distribution network integrated planning incorporating distributed generation and load response uncertainties," *IEEE Trans. Power Syst.*, vol. 26, no. 4, pp. 2164–2172, Nov. 2011.
[7] G. Celli, E. Giani, G. G. Soma, and F. Pilo, "Planning of reliable active distribution systems," *Int. Council Large Elect. Syst.*, 2012 Session, Paris, France, 2012.
[8] P. S. Georgilakis and N. D. Hatziargyriou, "A review of power distribution planning in the modern power systems era: Models methods and future research," *Elec. Power Syst. Res.*, vol. 121, pp. 89–100, 2015.
[9] S. S. Tanwar and D. K. Khatod, "A review on distribution network expansion planning," in *Proc. Annu. IEEE India Conf.*, 2015, pp. 1–6.
[10] J. Shu, L. Wu, Z. Li, and M. Shahidehpour, "A new method for spatial power network planning in complicated environments," *IEEE Trans. Power Syst.*, vol. 27, no. 1, pp. 381–389, Feb. 2012.
[11] S. Haffner, L. F. A. Pereira, L. A. Pereira, and L. S. Barreto, "Multistage model for distribution expansion planning with distributed generation—Part II: Numerical results," *IEEE Trans. Power Del.*, vol. 23, no. 2, pp. 924–929, Apr. 2008.
[12] S. Haffner, L. F. A. Pereira, L. A. Pereira, and L. S. Barreto, "Multistage model for distribution expansion planning with distributed generation—Part I: Problem formulation," *IEEE Trans. Power Del.*, vol. 23, no. 2, pp. 915–923, Apr. 2008.
[13] G. Muñoz-Delgado, J. Contreras, and J. M. Arroyo, "Joint expansion planning of distributed generation and distribution networks," *IEEE Trans. Power Syst.*, vol. 30, no. 5, pp. 2579–2590, Sep. 2015.
[14] A. Tabares, J. F. Franco, M. Lavorato, and M. J. Rider, "Multistage long-term expansion planning of electrical distribution systems considering multiple alternatives," *IEEE Trans. Power Syst.*, vol. 31, no. 3, pp. 1900–1914, May 2016.
[15] S. Najafi Ravadanegh, N. Jahanyari, A. Amini, and N. Taghizadeghan, "Smart distribution grid multistage expansion planning under load forecasting uncertainty," *IET Gener. Transmiss Distrib.*, vol. 10, no. 5, pp. 1136–1144, 2016.
[16] D. Rupolo, B. R. Pereira, J. Contreras, and J. R. S. Mantovani, "Medium- and low-voltage planning of radial electric power distribution systems considering reliability," *IET Gen., Transmiss Distrib.*, vol. 11, no. 9, pp. 2212–2221, 2017.
[17] R. Lotero and J. Contreras, "Distribution system planning with reliability," *IEEE Trans. Power Del.*, vol. 26, no. 4, pp. 2552–2562, Oct. 2011.
[18] E. Naderi, H. Seifi, and M. S. Sepasian, "A dynamic approach for distribution system planning considering distributed generation," *IEEE Trans. Power Del.*, vol. 27, no. 3, pp. 1313–1322, Jul. 2012.
[19] R. A. Jabr, R. Singh, and B. C. Pal, "Minimum loss network reconfiguration using mixed-integer convex programming," *IEEE Trans. Power Syst.*, vol. 27, no. 2, pp. 1106–1115, May 2012.
[20] G. Muñoz-Delgado, J. Contreras, and J. M. Arroyo, "Multistage generation and network expansion planning in distribution systems considering uncertainty and reliability," *IEEE Trans. Power Syst.*, vol. 31, no. 5, pp. 3715–3728, Sep. 2016.
[21] P. M. de Quevedo, G. Muñoz-Delgado, and J. Contreras, "Impact of electric vehicles on the expansion planning of distribution systems considering renewable energy, storage, and charging stations," *IEEE Trans. Smart Grid*, vol. 10, no. 1, pp. 794–804, Jan. 2019.
[22] J. M. Home-Ortiz, M. P. Kasmaei, M. Lehtonen, and J. R. S. Mantovani, "A mixed integer conic model for distribution expansion planning: Matheuristic approach," *IEEE Trans. Smart Grid*, vol. 11, no. 5, pp. 3932–3943, Sep. 2020.
[23] T. Ding, C. Li, Y. Yang, J. Jiang, Z. Bie, and F. Blaabjerg, "A two-stage robust optimization for centralized-optimal dispatch of photovoltaic inverters in active distribution networks," *IEEE Trans. Sustain. Energy*, vol. 8, no. 2, pp. 744–754, Apr. 2017.
[24] T. Ding, S. Liu, W. Yuan, Z. Bie, and B. Zeng, "A two-stage robust reactive power optimization considering uncertain wind power integration in active distribution networks," *IEEE Trans. Sustain. Energy*, vol. 7, no. 1, pp. 301–311, Jan. 2016.
[25] T. Ding, Y. Lin, G. Li, and Z. Bie, "A new model for resilient distribution systems by microgrids formation," *IEEE Trans. Power Syst.*, vol. 32, no. 5, pp. 4145–4147, Sep. 2017.
[26] S. Najafi, S. H. Hosseinian, M. Abedi, A. Vahidnia, and S. Abachezadeh, "A framework for optimal planning in large distribution networks," *IEEE Trans. Power Syst.*, vol. 24, no. 2, pp. 1019–1028, May 2009.
[27] J. E. Mendoza, M. E. López, S. C. Fingerhuth, H. E. Peña, and C. A. Salinas, "Low voltage distribution planning considering micro distributed generation," *Elec. Power Syst. Res.*, vol. 103, no. 8, pp. 233–240, 2013.
[28] C. Borges and V. Martins, "Multistage expansion planning for active distribution networks under demand and distributed generation uncertainties," *Int. J. Elec. P&E Syst.*, vol. 36, no. 1, pp. 107–116, 2012.
[29] V. Martins and C. Borges, "Active distribution network integrated planning incorporating distributed generation and load response uncertainties," *IEEE Trans. Power Syst.*, vol. 26, no.no. 4, pp. 2164–2172, Nov. 2011.
[30] D. Wang, L. Ochoa, and G. Harrison, "Modified GA and data envelopment analysis for multistage distribution network expansion planning under uncertainty," *IEEE Trans. Power Syst.*, vol. 26, no. 2, pp. 897–904, May 2011.
[31] N. C. Koutsoukis, P. S. Georgilakis, and N. D. Hatziargyriou, "Multistage coordinated planning of active distribution networks," *IEEE Trans. Power Syst.*, vol. 33, no. 1, pp. 32–44, Jan. 2018.
[32] D. Zhang, Z. Fu, and L. Zhang, "An improved TS algorithm for loss-minimum reconfiguration in large-scale distribution systems," *Elec. Power Syst. Res.*, vol. 77, no. 5, pp. 685–694, 2007.
[33] I. J. R. Rosado and J. A. D. Navarro, "New multi-objective Tabu search algorithm for fuzzy optimal planning of power distribution systems," *IEEE Trans. Power Syst.*, vol. 21, no. 1, pp. 224–233, Feb. 2006.
[34] B. R. Pereira Junior, A. M. Cossi, and J. Contreras, "Multiobjective multistage distribution system planning using Tabu search," *IET Gener. Transmiss. Distrib.*, vol. 8, no. 1, pp. 35–45, 2014.
[35] L. Zhao, Y. Huang, and Q. Dai, and *et al.*, "Multistage active distribution network planning with restricted operation scenario selection," *IEEE Access*, vol. 7, pp. 121067–121080, 2019.
[36] R. Li, W. Wang, and M. Xia, "Cooperative planning of active distribution system with renewable energy sources and energy storage systems," *IEEE Access*, vol. 6, pp. 5916–5926, 2017.
[37] S. Lei, Y. Hou, and F. Qiu, "Identification of critical switches for integrating renewable distributed generation by dynamic network reconfiguration," *IEEE Trans. Sustain. Energy*, vol. 9, no. 1, pp. 420–432, Jan. 2018.
[38] S. Montoya-Bueno, J. I. Muoz, and J. Contreras, "A stochastic investment model for renewable generation in distribution systems," *IEEE Trans. Sustain. Energy*, vol. 6, no. 4, pp. 1466–1474, Oct. 2015.
[39] J. M. H. Ortiz, M. P. Kasmaei, J. López, and J. R. S. Mantovani, "A stochastic mixed-integer conic programming model for distribution system expansion planning considering wind generation," *Energy Syst.*, vol. 9, no. 3, pp. 551–571, 2018.
[40] C. Zhang, J. Li, and Y. Zhang, "Optimal location planning of renewable distributed generation units in distribution networks: An analytical approach," *IEEE Trans. Power Syst.*, vol. 33, no. 3, pp. 2742–2753, May 2018.
[41] T. Ding, Y. Lin, Z. Bie, and C. Chen, "A resilient microgrid formation strategy for load restoration considering master-slave distributed generators and topology reconfiguration," *Appl. Energy*, vol. 199, pp. 205–216, 2017.
[42] J. A. Bondy and U. S. R. Murty, in *Graph Theory*. Berlin, Germany: Springer, 2008, vol. 311, no. 3, pp. 359–372.
[43] 1. T. Ding, Y. Lin, Z. Bie, and C. Chen, "A resilient microgrid formation strategy for load restoration considering master-slave distributed generators and topology reconfiguration," *Appl. Energy*, vol. 199, pp. 205–216, 2017.
[44] T. Ding, Y. Lin, G. Li, and Z. Bie, "A new model for resilient distribution systems by microgrids formation," *IEEE Trans. Power Syst.*, vol. 32, no. 5, pp. 4145–4147, Sep. 2017.
[45] T. Ding, Z. Wang, W. Jia, B. Chen, C. Chen, and M. Shahidehpour, "Multiperiod distribution system restoration with routing repair crews, mobile electric vehicles, and soft-open-point networked microgrids," *IEEE Trans. Smart Grid*, vol. 11, no. 6, pp. 4795–4808, Nov. 2020.
[46] H. Heitsch and W. Roemisch, "Scenario tree modeling for multistage stochastic programs," *Math. Prog.*, vol. 2, no. 118, pp. 371–406, 2009.
[47] A. Shapiro, D. Dentcheva, and A. Ruszczynski, in *Lectures On Stochastic Programming: Modeling and Theory*. Hoboken, NJ, USA: SIAM, 2009.
[48] J. Zou, S. Ahmed, and X. Sun, "Stochastic dual dynamic integer programming," *Math. Prog.*, vol. 175, pp. 461–502, 2019.
[49] R. Lu, T. Ding, B. Qin, J. Ma, X. Fang, and Z. Dong, "Multi-stage stochastic programming to joint economic dispatch for energy and reserve with uncertain renewable energy," *IEEE Trans. Sustain. Energy*, vol. 11, no. 3, pp. 1140–1151, Jul. 2020.
[50] J. Zou, S. Ahmed, and X. A. Sun, "Stochastic dual dynamic integer programming," *Math. Program.*, vol. 175, no. 1, pp. 461–502, May 2019.

[51] J. Zou, S. Ahmed, and X. Sun, “Multistage stochastic unit commitment using stochastic dual dynamic integer programming,” *IEEE. Trans. Power Syst.*, vol. 34, no. 3, pp. 1814–1823, May 2019.

[52] T. Ding, Y. Hu, and Z. Bie, “Multi-stage stochastic programming with nonanticipativity constraints for expansion of combined power and natural gas systems,” *IEEE Trans. Power Syst.*, vol. 33, no. 1, pp. 317–328, Jan. 2018.

[53] 2020. [Online]. Available: https://github.com/ZekaiWang-XJTU/data-of-33-bus-distribution-network

Tao Ding (Senior Member, IEEE) received the B.S.E.E. and M.S.E.E. degrees from Southeast University, Nanjing, China, in 2009 and 2012, respectively, and the Ph.D. degree from Tsinghua University, Beijing, China, in 2015. During 2013 and 2014, he was a Visiting Scholar with the Department of Electrical Engineering and Computer Science, University of Tennessee, Knoxville, TN, USA. During 2019 and 2020, he was a Visiting Scholar of the Robert W. Galvin Center for Electricity Innovation at the Illinois Institute of Technology. He is currently a Professor with the State Key Laboratory of Electrical Insulation and Power Equipment, the School of Electrical Engineering, Xi’an Jiaotong University. His current research interests include electricity markets, power system economics and optimization methods, and power system planning and reliability evaluation. Dr. Ding is an Editor of IEEE TRANSACTIONS ON POWER SYSTEMS, IEEE POWER ENGINEERING LETTERS, *IET Generation Transmission & Distribution* and *CSEE JPES*.

Ming Qu (Student Member, IEEE) received the B.S. degree from the School of Electrical Engineering, Shandong University, Jinan, China, in 2017. He is currently working toward the Ph.D. degree with Xi’an Jiaotong University. His major research interests include power system optimization and renewable energy integration.

Can Huang (Senior Member, IEEE) received the B.S.E.E degree from Hohai University, Nanjing, China, in 2008, the M.S.E.E. degree from Southeast University, Nanjing, China, in 2011, and the Ph.D. degree in electrical engineering from the University of Tennessee, Knoxville, TN, USA, in 2016. He is currently a Research Staff with Lawrence Livermore National Laboratory, Livermore, CA, USA. His current research interests include smart sensors, data analytics, and machine learning for energy and power systems, cyber-physical systems, and Internet of Things.

Zekai Wang (Student Member, IEEE) received the B.S. degree from the School of Electrical Engineering, Xi’an Jiaotong University, Xi’an, China, in 2018. He is currently working toward the M.S. degree with Xi’an Jiaotong University. His major research interests include power system optimization and resilience.

Pengwei Du (Senior Member, IEEE) received the Ph.D. degree in electric power engineering from Rensselaer Polytechnic Institute, Troy, NY, USA. He is currently with the Electric Reliability Council of Texas, Austin, TX, USA. Prior to this, he was a Senior Research Engineer with the Pacific Northwest National Laboratory, Department of Energy. He was the recipient of the IEEE PES Power System Dynamic Performance Committee Best Paper Prize in 2016 and the IEEE PES Best Paper Prize. He is also a Subject Editor of the *IET Generation Transmission and Distribution* and an Associate Editor for the IEEE TRANSACTIONS ON POWER SYSTEMS.

Mohammad Shahidehpour (Fellow, IEEE) received the Honorary Doctorate degree from the Polytechnic University of Bucharest, Bucharest, Romania, in 2009. He is the Bodine Chair Professor and Director of the Robert W. Galvin Center for Electricity Innovation at Illinois Institute of Technology. He is Fellow of the American Association for the Advancement of Science (AAAS), Fellow of the National Academy of Inventors (NAI), Laureate of KIA (Khwarizmi International Award), and an elected member of the US National Academy of Engineering. He is listed as a highly cited Researcher on the Web Science (ranked in the top 1% by citations demonstrating significant influence among his peers).